Membrane-substrate interface: Phospholipid bilayers at chemically and topographically structured surfaces

Atul N. Parikh[a)]
Department of Applied Science, University of California—Davis, Davis, California 95616

(Received 12 December 2007; accepted 7 February 2008; published 30 April 2008)

The surface-assisted fusion, rupture, and spreading of vesicles and hydration-induced spreading of lipids onto chemically and topographically structured surfaces gives rise to lipid structures useful for modeling many physical-chemical properties of lipid bilayers. Chemically structured surfaces produce a lipid structure revealing template-induced assembly of coexisting lipid phases, which reflect the underlying pattern of surface energy, wettability, and chemistry. In a construct derived using photochemically patterned molecular monolayers, the author found a spontaneous separation of fluid bilayer regions from the fluid monolayer regions by a controllable transition region or moat. The coexisting bilayer/monolayer morphologies derived from single vesicular sources are particularly attractive for the study of a range of leaflet-dependent biophysical phenomena and offer a new self-assembly strategy for synthesizing large-scale arrays of functional bilayer specific substructures including ion-channels and membrane-proteins. The uses of topologically patterned surfaces similarly provide new models to design complex three-dimensional membrane topographies and curvatures. These platforms promise fundamental biophysical studies of curvature-dependent membrane processes as well as useful bioanalytical devices for molecular separations within fluid amphiphilic membrane environments. Some future directions enabled by lipid self-assembly at structured surfaces are also discussed. © *2008 American Vacuum Society.* [DOI: 10.1116/1.2889055]

I. INTRODUCTION

From a surface science perspective, supported membranes represent a class of bimolecular interfacial films consisting of two opposing monolayers of phospholipids supported at the aqueous interfaces of hydrophilic solids.[1,2] Continued interest in these systems stems primarily from their usefulness as simplified model systems for developing a physical-chemical understanding of many reaction-diffusion processes that characterize structure, assembly, dynamics, and functions of complex, heterogeneous biological membranes.[3–5] Some broad classes of inquiries where supported membranes have proved useful include phase stability and dynamics (e.g., lipid-lipid phase separation, raft formation, and lateral diffusion), protein-membrane interactions (e.g., receptor clustering and co-localization, pattern formation, and pore formation), and membrane-membrane processes such as fusion and adhesion and intercellular recognitions.[3,4,6] Moreover, because supported membranes integrate a fluid phospholipid structure with a solid surface, which in turn may serve as a transducer of membrane processes (e.g., resistance to nonspecific binding, specific protein-receptor bindings, and trans-membrane transport), they are also relevant to the design of synthetic biocompatible surfaces, membrane-based biosensors and devices, and analytical platforms for assaying membrane-based processes.[3,7,8]

Supported membranes are typically formed at the solid-liquid interface when vesicular microphases of lipids and their mixtures rupture and spread spontaneously on hydrophilic surfaces (Fig. 1).[9–11] Alternatively, they can be formed by two successive transfers of lipid monolayers from the air-water interface onto planar surfaces such as silica or mica (Langmuir-Blodgett methods),[12] or by using hydrated lipid stacks, which spread upon hydration (lipid spreading methods).[13–15] When appropriately formed, these substrate-supported bilayers are separated from the substrate surface through an intervening cushion layer (e.g., a hydration layer of water variously estimated between 6 and 15 Å thick),[16] in equilibrium with its bulk surrounding on the opposite side of the bilayer. While the details of the properties of the substrate-bound hydration layer at the membrane-substrate interface remain incompletely characterized,[17] many previous theoretical and experimental studies of water in confinement and near their interphases with polar hydrophilic surfaces suggest that it is more ordered with higher viscosity and lower dielectric constants.[18] Consistent with these predictions, many examples now confirm that characteristics of the lipid bilayer remain structurally coupled with essential substrate properties (e.g., charge, wettability, and topography). The coupling is manifest in several ways including, for instance, (1) substrate-charge induced overall and leaflet-dependent compositional asymmetry in supported bilayers compared to their parent vesicles;[19] (2) wettability-induced membrane morphologies;[20,21] and (3) varying degree of frictional coupling of at least the proximal (near-substrate) leaflet of the bilayer.[22] Some recent studies also suggest independent melting characteristics for the two proximal and the distal leaflets of bilayers when they cross their gel-fluid transition temperatures.[23]

a)Electronic mail: anparikh@ucdavis.edu

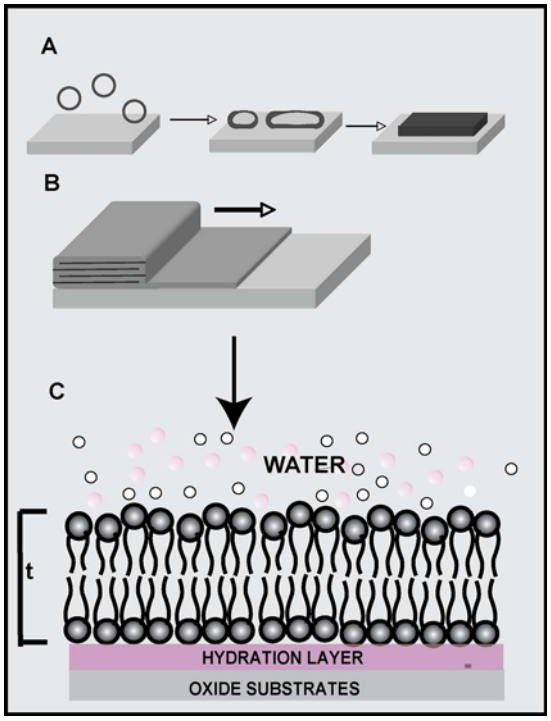

FIG. 1. Surface self-assembly of lipid bilayers. Schematic illustration of popular methods for forming lipid bilayers at hydrophilic surfaces. (A) Adsorption, rupture, and spreading of lipid vesicles and (B) hydration-induced spreading of single bimolecular lipid films. (C) Cartoon showing an idealized single bilayer structure of thickness t in 4–6 nm range, obtained by these methods.

A dominant focus over the past several decades, in this regard, has been to develop strategies to efficiently decouple substrate-membrane interactions. A central driving force for this focus is that the native hydration layer is insufficient in thickness to eliminate contacts between membrane proteins with large extra-membrane domains and substrate. Such contacts may frustrate the conformational and translational dynamics required to reconstitute protein functions within supported membrane configuration.[2,24] Moreover, as noted above, there is also a growing appreciation that frictional or electrostatic coupling between the substrate and at least the proximal leaflet of the lipid bilayer may introduce undesirable asymmetries in structural, compositional, mechanical (e.g., drag), and dynamical properties of supported membranes. To this end, a variety of approaches aimed at cushioning the membrane-substrate interphase region have proved successful. Using intermediate or intercalated "soft" cushioning layers of water in the 10–100 nm thickness range by incorporating hydrophilic tethers, hydrogels, and polymeric cushion all have proved successful.[2,25]

The notion that deliberate coupling of substrate properties with a membrane bilayer can produce potentially useful templated membrane configurations has, in contrast, received much less attention. Because the roles of many substrate properties (e.g., substrate wettability, charge, and topography) that influence membrane formation are beginning to be well understood,[9,11] it appears that a careful control of substrate properties can provide simple and effective means to *template* many membrane properties including spatial molecular distributions and compositional heterogeneities, lateral tension, packing density, curvature, and even membrane morphologies. Moreover, recent advances in patterning and surface modification methods[26,27] (chemical and topological) allow fabricating substrate surfaces that exhibit an unprecedented level of control of spatial variations in substrate properties at micro- to nanometer length scales. Use of such structured surfaces then provides a means to *locally* vary substrate-membrane interactions, which in turn should template coexisting surface patterns of membrane properties within single bilayers. These opportunities are beginning to be explored.[20,21,28] *Here, we review a collection of such efforts from our laboratory and elsewhere, which illustrate deliberate substrate-membrane coupling using simple structured surfaces exhibiting binary chemical and topographic corrugations.* Note that the efforts highlighted here merely illustrate, rather than comprehensively survey, many studies in the literature that contribute to this notion.

II. MEMBRANES AT CHEMICALLY STRUCTURED SURFACES

Surface chemisorption or molecular self-assembly is an elegant route to preparing chemically structured surfaces. Both major classes of self-assembling systems, namely alkanethiols on coinage metals[29,30] (e.g., Au, Ag, and Cu) and alkylsiloxanes on oxide substrates[31] (e.g., SiO_2), are amenable to spatial chemical patterning spanning nanometer to micrometer scale feature dimensions over macroscopic sample areas. A variety of patterning techniques including optical lithographies, micro-contact printing based methods, dip-pen nanolithography, ink-jet printing, and others have proved remarkably useful for the creation of chemically corrugated surfaces.[27,32,33] From a membrane organization (e.g., vesicle fusion or lipid spreading) point of view, such chemical corrugation at substrate surfaces provides one of the most convenient ways to design patterns of (1) surface charge, (2) membrane-surface adhesion energy, (3) interfacial energy or wettability, and (4) shallow topographic textures (<2 nm). Below, we illustrate the use of chemically corrugated surfaces to spatially modulate interfacial energy (or wettability) and its role in templating lipid self-assembly.

It has been recognized for some time that substrate interfacial energy[34,35] plays an important role in determining vesicle spreading behavior and the resulting surface-bound lipid phases. At hydrophilic surfaces, exposure of small unilamellar vesicles (SUVs) results in the formation of single phospholipid bilayers[13] via somewhat better understood vesicle rupture and spreading mechanisms.[9] Examples of hydrophilic substrates that promote successful bilayer formation include freshly oxidized surfaces of glass, quartz, mica, and silicon wafers. Note that not all hydrophilic surfaces promote vesicle fusion. Surfaces of oxidized metals and metal-oxides (e.g., TiO_2, Pt, and Au) allow adsorption of intact vesicles but resist the formation of bilayers presumably because of weak surface interactions.[36] Hydrophobic supports, on the other hand, foster vesicle spreading by a

different mechanism which consistently produces single phospholipid monolayers.[30,31,35,37] In reconciling these observations in the context of structured surfaces, a number of general questions naturally arise. *First*, do structured surfaces locally template and modulate vesicle fusion and lipid spreading mechanisms if the support surfaces display microscopic regions of hydrophilic and hydrophobic character? Such a templating mechanism should produce coexisting regions of lipid mono- and bilayers from single parent stock in single samples. Such composite surfaces would be of considerable interest as models for direct comparisons of membrane functions that require correspondence between the two leaflets of the bilayer architecture. Furthermore, from a practical view point, many hydrophilic surfaces used for bilayer formation are easily contaminated by adventitious organics[38] and thus display surface chemical and wettability heterogeneities. How such heterogeneities impact bilayer integrity appears related. *Second*, are there lower thresholds for the local surface-energy-dependent control of bilayer formation mechanisms? It appears intriguing to determine how surface templating manifests when the length scales at which substrate properties are varied become shorter than the "persistence length" of lipid self-assembly determined probably by the synergy of lipid-lipid van der Waals interactions and hydrophobic effect. Such an interplay between spontaneous self-assembly of lipids and surface-mediated templating should also produce interesting lipid patterns and suggest new routes to directing self-assembly processes.[39] Recently, theoretical studies by Andelman and co-workers[40] have examined the role of spatially modulated membrane-substrate interaction using mean-field theories. These studies predict improved adhesion between fused planar bilayers and substrates at chemically patterned, periodic surfaces, but suggest complex morphologies determined by a delicate balance between adhesion, bending, and tension at structurally or chemically rough heterogeneous surfaces. Experimental validations of these predictions are also not available. *Third*, how do lipids organize at the *interphase* between hydrophilic and hydrophobic regions? If the *interphase* region were smaller than the threshold values discussed above, how would lipid transition from, for instance, mono- to bilayers such as during spreading at hydrophobic surfaces textured with hydrophilic "defect" regions? These questions are of course not limited to specific lipid systems and addressing them should yield useful insights into how surfaces can be used to template lipid organization at surfaces and elaborate available model systems to study biophysical chemistry of lipid bilayers.

In a recent study,[20] we have shown that mixed hydrophilic/hydrophobic surfaces, displaying prepatterned variations of interfacial energies separated by a lipophobic *interphase*, can template vesicle fusion mechanisms. This surface templating gives rise to well-separated coexisting fluid-fluid morphologies that reflect the underlying pattern of substrate wettability. The substrates were produced by combining silane self-assembly with photochemical patterning to create binary surfaces displaying hydrophilic and hydrophobic regions separated by a topochemically roughened *interphase* region. Specifically, we *used* ozone-generating short-wavelength ultraviolet (UV) radiation and a physical mask for directing UV illumination to pattern *n*-octadecyl trichlorosilane (OTS) monolayers on glass and oxidized silicon substrates.[41,42] Preassembled OTS monolayers, prepared by following a standard solution self-assembly procedure,[43] are patterned using an ozone generating short-wavelength ultraviolet radiation (184–257 nm) in conjunction with a photomask.[42] The treatment results in binary surface energy patterns comprising intact OTS in UV-protected regions (hydrophobic) and oxidized silica in the UV-exposed regions (hydrophilic). Simple condensation figures, such as derived by selective vapor depositions[44] and ellipsometry, confirm the patterned hydrophilic/hydrophobic character of the resulting surfaces. We then investigate the spreading of small unilamellar vesicles (SUVs) composed of POPC (1-Palmitoyl-2-oleoyl-*sn*-glycero-3-phosphocholine) vesicles doped with 1 mol % Texas-Red-labeled DHPE (Texas Red® 1,2-dihexadecanoyl-*sn*-glycero-3-phosphoethanol-amine, triethylammonium salt, TR-DHPE) onto such surfaces (Fig. 2). The observed fluorescence pattern is in excellent correspondence with that of surface wetting character in the underlying template. Three regions of distinctly different fluorescence intensities are discernible: (1) a bright fluorescent region corresponding to the hydrophilic parts of the pattern, (2) a weaker fluorescent surrounding corresponding to the hydrophobic parts, and (3) a transition region separating the two regions above. Fluorescence recovery after photobleaching (FRAP) measurements[45] confirm the fluidity of each lipid mono- and bilayer region of the composite sample. To test if the two mono- and bilayer fluids are connected, spot sizes comparable to that of the corralled lipid bilayer (or the monolayer) region were first photobleached. Over time, the bleached molecules remain confined within the corralled phase and did not spread from the patterned element to the surrounding areas.[20] Taken together, these simple experiments establish that within each contiguous morphological feature, diffusive mixing occurs, but there is little or no intermixing between the adjacent mono- and bilayer fluids across the moat region.

Lipid spreading[13,14] is another proven methodology often used to prepare supported membrane configurations. To examine how structured surfaces influence lipid spreading behavior, we performed a spreading experiment using real-time fluorescence and imaging ellipsometry characterization.[13,14,46] Briefly, POPC lipids (doped with a 2% concentration of Texas Red DHPE probe) are dried onto the thin edge of a glass slide from their chloroform solution. Subsequently, the nominally dried lipid cake is transferred to a patterned OTS surface (prepared as above) by bringing the two surfaces in contact for 5–10 s. The unhydrated bulk lipid is stamped symmetrically about the pattern features so that spreading on both the hydrophilic and hydrophobic surface can be simultaneously observed. The sample is then positioned within a fluorescence microscope and the lipid cake hydrated by flooding the surface with a small amount (3–5

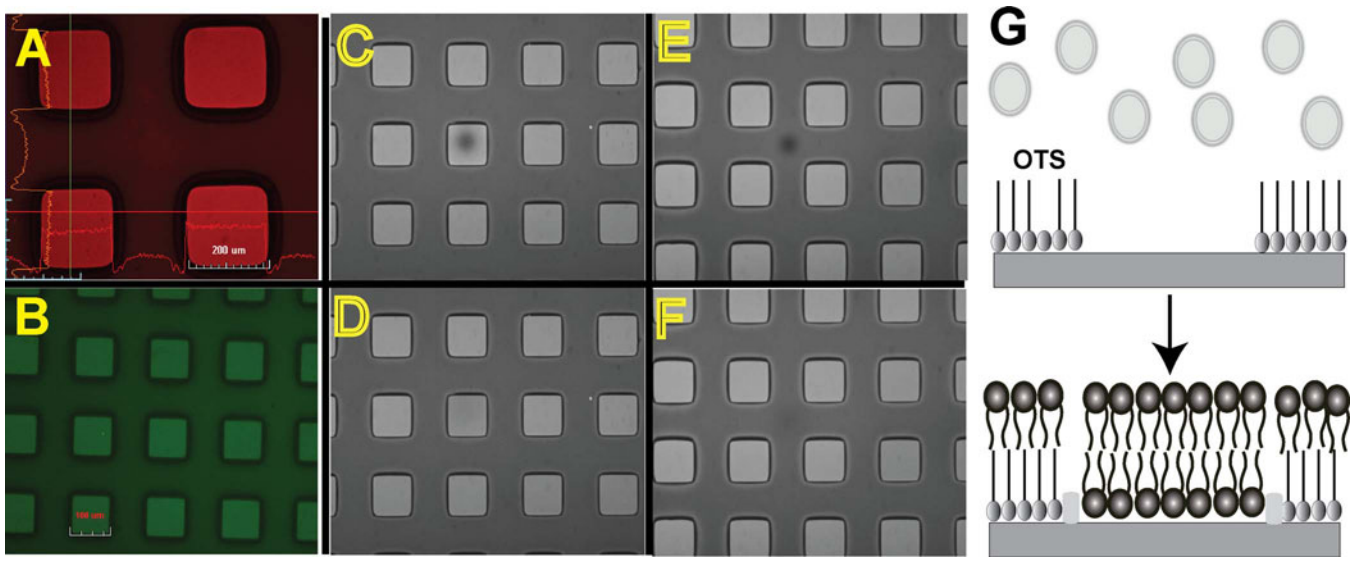

FIG. 2. Coexisting lipid mono- and bilayer morphologies templated by surface energy patterns. (A) Epifluorescence microscopy image (10×) and the corresponding intensity line scan of the surface-templated POPC lipid (doped with 1 mol % TR-DHPE) organized as bilayer (bright squares) and monolayer regions in hydrophilic and hydrophobic regions, respectively. (B) Same as (A) for DMPC bilayer doped with 1 mol % NBD-DHPE. (C–F) Recovery of photobleached spots in bilayer (C,D) and monolayer (E,F) regions of the sample. The images are taken approximately 12 min apart. (G) A schematic depiction of vesicle fusion onto a patterned hydrophilic/hydrophobic surface. The spacer region between the mono- and bilayer morphology suggests the topochemically roughened boundary region of ill-characterized width and surface properties. (For details, see Ref. 20.)

ml) of de-ionized water at room temperature. The time sequence of images (Fig. 3) reveals a rapid spread as seen by a bright fluorescent front moving away from the lipid source. Within several minutes, the spreading is complete as signaled by the equilibrated fluorescence morphology comparable to those observed by vesicle fusion in Fig. 2. Ellipsometric images shown in Fig. 3 further confirm that the spreading results in the formation of single bilayers in the hydrophilic regions and a single monolayer in the OTS regions of the patterned substrate. We also see that the two spreading processes occur in parallel, albeit monolayer, spreads at considerably faster rates than the bilayers on hydrophilic surfaces, presumably reflecting the differences in spreading energetics. In good agreement with vesicle fusion derived membrane

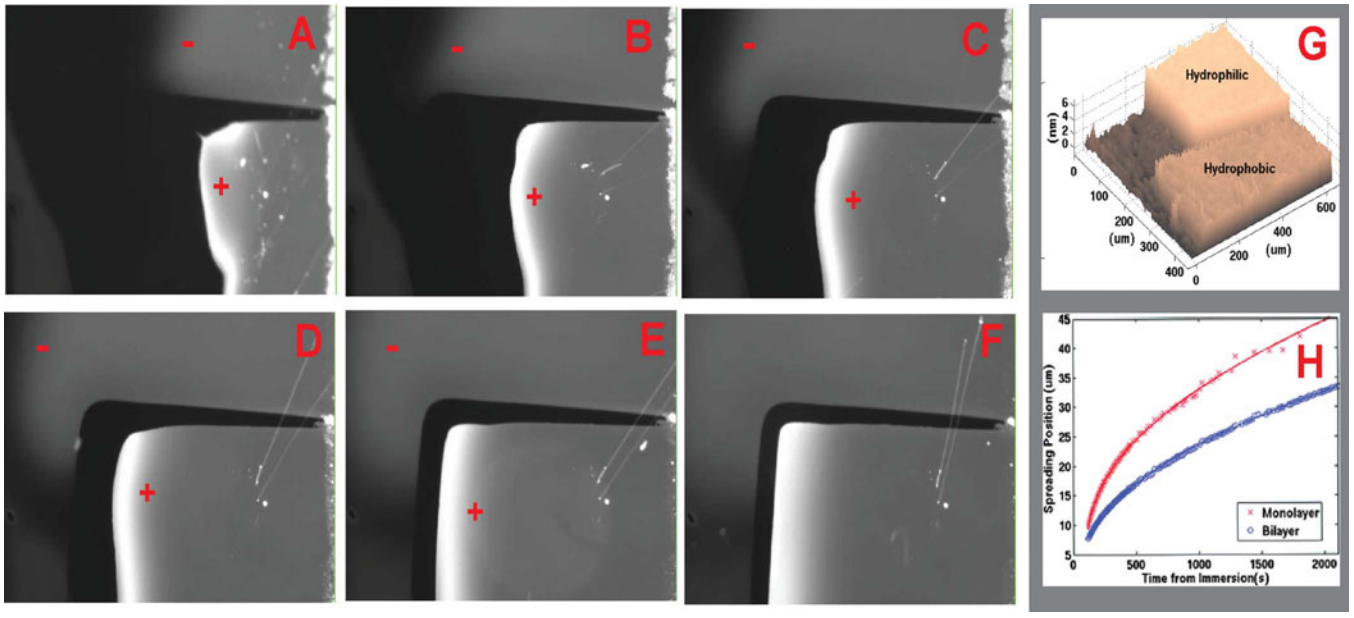

FIG. 3. Hydration-induced spreading of lipids at structured surfaces. (A–F) Arbitrarily chosen frames from a time-lapse fluorescence movie of lipid spreading on a patterned OTS surface. The images span 20 min following initial hydration. The lipid source is stamped at the right edge of each image. The spreading occurs on both hydrophobic and hydrophilic regions in parallel with lipid monolayer spreading considerably faster on the hydrophobic regions. (G) Ellipsometric thickness map confirms the formation of a single bilayer on hydrophilic and a single monolayer on hydrophobic regions of the sample. (h) The time-evolution positions of lipid fronts for hydrophobic (red) and hydrophilic (blue) confirm faster spreading of the monolayers. (For details, Ref. 15.)

configurations, the mono- and bilayer phases remain distinct without any measurable exchange of molecules between the two morphologies.

Together, these experiments indicate that local variations in substrate wettability control both the lipid spreading and vesicle fusion mechanisms at structured surfaces: hydrophilic regions prompt the bilayer formation whereas monolayers form on hydrophobic regions within single samples. In the examples presented here, the use of photopatterned OTS surfaces gives rise to spontaneous corralling of single, fluid lipid bilayers in hydrophilic regions from the surrounding fluid monolayers formed in the hydrophobic region. The two mono- and bilayer lipid morphologies are separated by a lipid-free transition region, which corresponds to the topochemically roughened interphase of the starting substrate. These examples pose several intriguing questions regarding substrate templating of vesicle fusion and lipid spreading: (1) How do spatial gradients in surface energy (and wettability) template lipid self-assembly? (2) What sort of diffusive transport occurs if the lipid mono- and bilayers are contiguous when substrates do not present non-fusogenic transition moats? Do only molecules present in the outer leaflet of the bilayer exchange with the adjacent monolayer, thus confining lipids in the lower leaflet of the bilayer? Do defects allow lower leaflet molecules to flip-flop and allow complete compositional equilibrium between the mono- and bilayers? (3) Do monolayers spontaneous interconvert to bilayers (and vice versa) as lipids spread over alternating hydrophilic and hydrophobic substrate regions? What are the energetic needs for such large-scale structural reorganizations? (4) How small a hydrophilic (or hydrophobic) region can prompt switch in self-assembly mechanisms? In other words, what are the thresholds for local surface-energy control of lipid spreading and vesicle fusion mechanisms? These questions (and others not discussed above) suggest interesting new opportunities in understanding membrane-substrate interactions (e.g., adhesion energy) and its interplay with lipid-lipid (e.g., van der Waals) and lipid-solvent (e.g., hydrophobic effect) interactions in directing membrane formation at solid surfaces.

III. APPLICATIONS OF PATTERNED MORPHOLOGY LIPID SUBSTRATES

The juxtaposition and spontaneous corralling of lipid mono- and bilayer morphologies, achieved in single samples from a single vesicular source using photopatterned silane substrates, provide a useful and generic platform. For instance, the platform enables comparing, probing, and quantifying the roles of two-leaflet cooperativity in controlling membrane physical chemical characteristics (e.g., elastic responses, thermodynamic transitions, phase separations, and pattern formation) and promises new routes to pattern membrane-associated functions. The variety of applications is illustrated below using two recent examples where we study the (1) differences in mono- and bilayer responses to local and nonspecific adhesive interaction suggesting the effects of interleaflet processes on membrane mechanical properties and (2) confinement of ion-channel induced transport to bilayer regions of the pattern illustrating the use of the platform for patterning membrane associated functions.

A. Comparing elastic responses of lipid mono- and bilayers to local adhesive interactions

The interaction between supported, fluid lipid membranes and microscopic colloids[47] is regarded as a simplified physical model for understanding the role of membrane elasticity on biologically important mechanisms, e.g., particle engulfment, membrane fusion, and viral budding.[47,48] Previous theoretical efforts establish that the elastic response of the membrane is determined by a balance between the adhesion, tension, and bending energies.[49] Previous experiments have focused primarily on the interaction between "free" membranes of giant phospholipid vesicles (>10 μm) and latex microspheres.[50] Notable limitations of giant vesicles in modeling particle adhesion at biological membranes include their vanishingly low lateral tension and the presence of large, out-of-plane undulations.[51,52] At cellular surfaces, however, the cytoskeleton constraints, the presence of trans-membrane proteins, and even compositional asymmetries renormalize membrane tension and limit the cooperativity in the natural dynamics of the two leaflets.[53] Because lipid monolayers supported on OTS surfaces (see above) experience a rigid hydrophobic interface with the substrate, its elastic response is confined to a single leaflet, thus providing a limiting case for decoupling dynamics between the two membrane leaflets.

In a recent study,[54] we presented microscopic, bare glass beads to binary patterns comprising alternate regions of lipid monolayers and bilayers.[20] Bright field optical data, reproduced in Fig. 4 (top panel), show that beads settle uniformly over the entire surface. Epifluorescence images also shown in Fig. 4 reveal an additional distinction between the beads adhering to bilayer and monolayer regions when the lipid layers are above the bulk transition temperature (24 °C). A fixed number of beads in the fluid bilayer regions appear roughly four times more fluorescent, suggesting a near-complete wrapping of the beads by the underlying membrane bilayer.[55] A rough calculation indicates $\sim 6\% - 8\%$ expansion of the projected surface area due to membrane wrapping around the adhering beads. Further, fluorescence recovery after photobleaching (FRAP) measurements in the vicinity of the fluorescent beads reveal two additional aspects of the colloid-membrane complex: (1) the lateral probe diffusivity of the membrane, a measure of membrane fluidity, appears to remain essentially unchanged before and after bead adhesion and (2) the membrane wrapped around the beads is essentially continuous with the underlying supported bilayer. In contrast, no such fluorescence acquisition by beads or membrane wrapping was seen in the monolayer regions (Fig. 4). Together, these simple experiments suggest that the adsorption of glass beads to fluid lipid membranes can be used as a simple means to differentiate local morphologies, viz., lipid bilayers from monolayers and voids or defects. The qualitatively different responses to bead adhesion by symmetric bi-

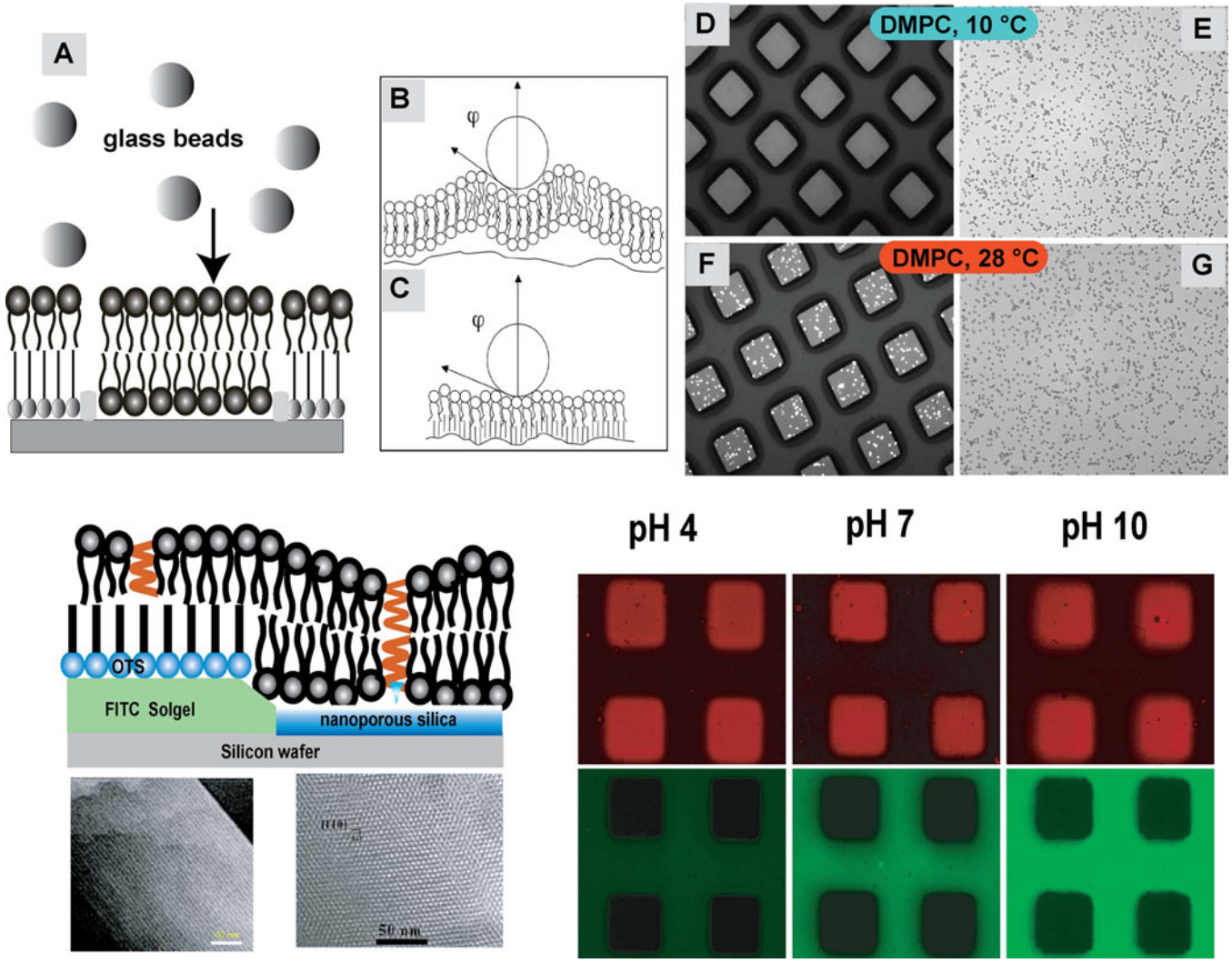

FIG. 4. Applications of patterned lipid morphologies. (Top) Cartoon illustration of bead settling onto patterned lipid mono- and bilayer construct. Note that the width of the boundary between the mono- and the bilayer regions remains ill- characterized. It is unlikely to be molecularly sharp because of penumbral blurring during substrate photopatterning (see text for details). (B,C) Cartoons illustrating (B) bead wetting or membrane wrapping for bilayers and (C) nonwetting for OTS supported monolayer regions. (D–G) Fluorescence (D,F) and optical images (E,G) of membrane-bead assembly for DMPC layers below [10 °C (D,E)] and above [28 °C (F,G)] the transition temperature (24 °C). (For details, see Ref. 54.) (Bottom) Patterning of ion-channel induced proton transport using mono- and bilayer constructs using POPC bilayer doped with 0.1% gramicidin. Selective dimerization of gramicidin in bilayer region allows proton equilibration between the membrane-nanoporous substrate interface and the ambient bulk. The sevenfold change in fluorescein intensity in the doped sol-gel silica substrate as ambient *p*H is varied from 4 to 10 provides striking evidence for optical transduction of the transmembrane proton transport. (For details, see Ref. 56.)

layers and asymmetric, OTS supported lipid monolayers also provide useful insights into elastic properties of supported membranes. *First*, for lipid monolayers supported on OTS, the lower leaflet equivalent, namely OTS, is directly tethered to the substrate. As a result, the "unbinding" of lipid monolayers required to wrap around the beads must impose a high hydrophobic penalty through the requisite separation at the hydrophobic mid-plane and can therefore be expected to be strongly suppressed. Our results are entirely consistent with this picture and provide a practical *caveat* against direct comparisons of adhesive responses of mono- and bilayer based models. They further suggest that the interactions between the inner leaflet of biological membranes and the cytoskeleton may modulate the membrane's elastic response to local deformation. These experiments also suggest, albeit much more work is needed, that it may be possible to probe elasticity of supported membranes in spatially resolved manners simply by introducing glass beads and quantifying the number and extent of bead wrapping. Such work is currently in progress.

B. Patterning ion-channel transport using structured membrane morphologies

From bioanalytical or biomimetic perspective, coexisting but isolated lipid structures afforded by photochemically patterned OTS monolayers should allow bilayer (or monolayer) specific membrane functions to be spatially localized and patterned into functional arrays. An example of such patternability was recently demonstrated using a patterned thin-film

silica mesophase substrate consisting of alternating hydrophilic nanoporous regions and hydrophobic nanostructured regions.[56] It was shown that interleaflet dimerization of gramicidin in lipid bilayers, and the absence of such dimerization possibility in adjacent lipid monolayers, allows for spatially localized transport of protons. To enable direct characterization of proton transport, we used the complex mesophase structure wherein the adjoining OTS derivatized mesostructure is doped with a fast-response *p*H sensitive probe.

Our design, illustrated in Fig. 4 (bottom panel), consists essentially of the functional "transporter" region and surrounding "reporter" region. The transporter region consists of a hydrophilic, mesoporous silica region of a patterned thin film supporting a complete lipid bilayer incorporating gramicidin, a short helical polypeptide, in both leaflets of the fluid bilayer. The presence of the gramicidin sequence in each leaflet permits ion-channel formation via lateral diffusion and interleaflet dimerization for subsequent proton transport.[57] An adjoining reporter region that reports on *p*H changes surrounds each transporter region. These reporter, or transduction, areas consist of the fast-response, *p*H-sensitive dye fluorescein isothiocyanate (FITC) embedded in a mesostructured, surfactant-containing, silica film.[58] In these regions, membrane transport functions are blocked by the presence of the OTS monolayer on the surface of the silica mesophase. The use of photochemically patterned thin films and OTS[59] allows for spatial separation of the reporter region and the transporter region via the transition moat regions as discussed above. Fluorescence microscopy data summarized in Fig. 4 (bottom panel) summarize the spatial confinement (and optical reporting) of gramicidin transport. Fluorescence images obtained using a red emission filter, appropriate for Texas Red DHPE, establish the stability, integrity, and structural consistency of the bilayer in aqueous media at the three *p*H values examined. The adjustment of aqueous phase *p*H values was achieved simply by adding controlled amounts of HCl or NaOH to the aqueous phase. Images obtained using a green emission filter appropriate for FITC reveal substantial changes in emission intensity from the reporter region in the presence of gramicidin, with an increase of more than a factor of 7 observed between *p*H values of 4 and 10. In contrast, control experiments confirm that only small changes in FITC emission occur for POPC samples devoid of gramicidin.[56]

The example above clearly demonstrates the localization and patterning of ion-channel transport in bilayer specific regions. It also confirms the usefulness of substrate chemical corrugation (namely patterned OTS surface in the present case) in controlling membrane-associated functions (e. g., transport in the present case). It seems reasonable that other membrane proteins (e.g., GPCRs) can also be selectively intercalated into bilayer regions alone, thereby allowing their specific functions (e.g., protein or drug binding) to be spatially compartmentalized and patterned. The generality of the approach should allow arraying the multi-functional reporter/transporter unit in a high-density format, thus facilitating parallel, on-chip, and high-throughput studies of ion-channels and membrane proteins.[8]

IV. MEMBRANES AT TOPOGRAPHICALLY STRUCTURED SURFACES

A variety of micro- and nanolithographic as well as self-assembly and sot-lithography based methods are now available to controllably induce surface topographic features over a broad range of feature dimensions.[26,33,60] Such surfaces can be used to template complex shapes and curvature patterns for compliant lipid bilayers. Recently, several reports have appeared where nanolithographically structured surfaces have been shown to impose complex topographies on lipid bilayers.[61–63] Below we illustrate two simple, convenient, nonlithographic, and cost-effective methods to achieve complex three-dimensional substrate topographies suitable for supporting compliant lipid bilayers.

First, many soft and elastomeric materials undergo structural failures and produce surface wrinklings[64,65] in strikingly uniform manners over large macroscopic areas. Understanding of the formation mechanisms for such instabilities now enables the design of well-defined patterns of surface topographies, such as buckles, bristles, and wrinkles, in predictable manners. For instance, releasing uniaxially stretched elastomers (e.g., polydimethyl siloxanes, PDMS) after surface oxidation produces multiple nested orders of periodic surface curvatures over macroscopic areas of the elastomeric surface.[65] Here, a thin surface layer ($\sim$5 nm) of the elastomer undergoes oxidation forming a strain-free and equilibrated stiff surface "skin." The oxidative process renders the PDMS surface hydrophilic, composed essentially of silica,[66] whereas the underlying bulk remains elastomeric and under strain. The difference in the equilibrium strains in the two layers gives rise to surface wrinkle formation when the stretch is released. The largest period so produced is $\sim$18 μm and the smallest period, embedded hierarchically, is $\sim$80 nm. This nested hierarchy of wrinkles forms because of the mismatch in equilibrium strains of the skin and the underlying elastic substrate.[65] While still in the stretched configuration, the newly formed skin is equilibrated while the bulk remains under tensile stress. Removing the stretch exerts a compressive strain on the skin that gives rise to a bending-dominated deformation, forming the smallest wavelength wrinkles. The saturation of the amplitude of the smallest wavelength wrinkle may give rise to higher order wrinkles determined by the competition between the bending-dominated deformation of the skin and the stretching-dominated response of the underlying PDMS.[65] Thus by controlling the initial extension and the rate of release, a variety of surface structures and length scales can be produced.[67] In addition to uniaxial stretches, other stretch geometries (e.g., radial and hexagonal) can be used to produce more complex, two-dimensional surface periodicities and are similarly tunable.[68]

As illustrated in Fig. 5, the ability of phospholipid bilayers to self-assemble in a topology prescribed by the curvature patterns of the underlying wrinkled elastomer is now established using both vesicle fusion and lipid spreading methods.[69] Epifluorescence microscopy reveals a homogeneous fluorescence emission formed interrupted by enhanced

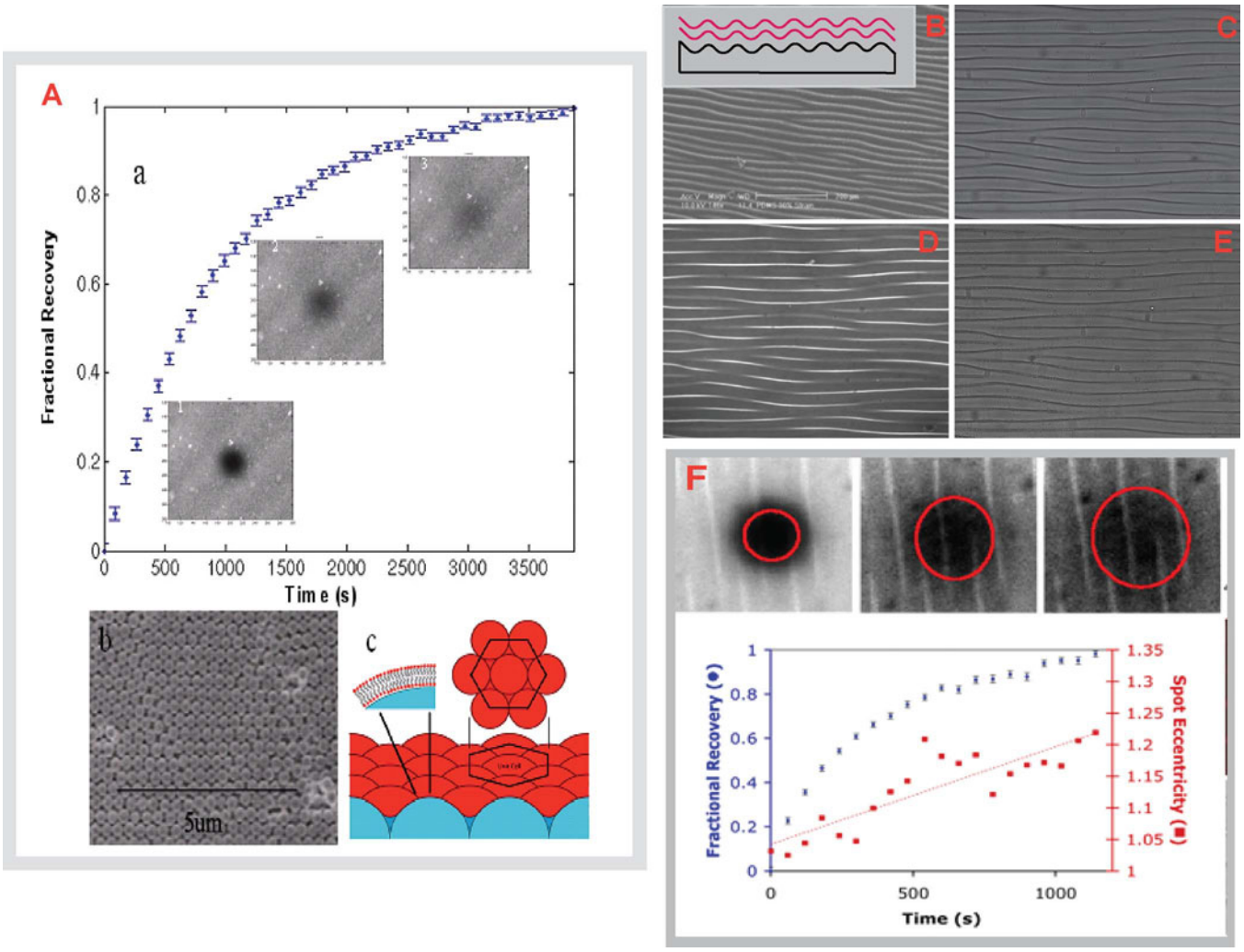

FIG. 5. Membranes on topographically structured surfaces. (A) (Top) FRAP fractional recovery plot of a Texas-Red-doped POPC bilayer on a 330 nm colloidal crystal. Insets: 200×160 μm^2 epifluorescence images of bleached spot (40 μm diameter) at times $t=0$, 630, and 1530 s. (Bottom left) SEM image of a 330 nm silica colloidal crystal. (Bottom right) Cartoon illustrating a compliant lipid bilayer (red) on top of a colloidal crystal (blue). (B–E) SEM image of a wrinkled PDMS elastomer (B), bright field optical image of the elastomer supporting a POPC bilayer in water (C), and fluorescence images for the POPC bilayer with gravitationally settled 1 μm glass beads. (F) Anisotropic recovery of a photobleached spot in FRAP confirms membrane undulation comparable to that of the underlying substrate.

parallel streaks of greater fluorescence emission for POPC bilayers doped with 1 mol % TR-DHPE. The observed fluorescence pattern corresponds well with the features observed in bright field transmission images (Fig. 5). Large silica beads (1 and 5 μm diameter) introduced into the aqueous phase and allowed to gravitationally settle colocalize with these features, establishing that these streaks further correspond to grooves (or valleys) of the wrinkle topography. The enhanced fluorescence intensity near the grooves is consistent with a greater lipid density projected onto the image plane by the curved substrate topography, probably also modulated by a different lipid micro-environment within the grooves. That the membrane roughly follows substrate topography is further substantiated by quantitatively analyzing the anisotropic recovery profile of a photobleached spot in a FRAP experiment. An examination of the time-lapse movie of the fluorescence recovery dynamics (Fig. 5) reveals that the initial circular morphology of the photobleached spot transitions into an elliptical one. The observed ellipse is oriented with its major axis aligned parallel to the grooves of the wrinkles, suggesting that the membrane must at least partially follow the substrate topography. The asymptotic value of the observed time-dependent spot eccentricity together with an independent characterization of the substrate topography by AFM suggests that the membrane follows the largest wrinkle period, albeit partial adherence to higher order wrinkles may also occur. These results are described in detail elsewhere.[69]

Second, in this same vein, the ability of monodisperse colloids to spontaneously organize into a face-centered cubic (fcc) lattice[70,71] provides another simple self-assembly route for the design of surfaces that exhibit periodic spatial variation in single and uniform two-dimensional (2D) curvatures. Colloids in a broad range of sizes from hundreds of nanometers to several micrometers can be used to produce the corresponding range of 2D curvatures. We have recently

adapted the popular physical confinement methods[72] wherein slow solvent evaporation drives the formation of 2D and 3D planar colloidal crystals from their aqueous sols using glass and polystyrene colloids.[73] Recent advances in the synthesis of asymmetrically shaped colloids and abilities to organize them at surfaces in controlled geometries may also allow generation of complex shapes and Gaussian curvature topologies wherein the two principle radii of curvature are inequivalent.[71,74]

As above, both vesicle fusion and lipid spreading methods appear to form homogeneous single bilayers on colloidal crystals. The observed bright and homogeneous fluorescence signal [Fig. 5(a) insets] indicates the formation of a laterally uniform POPC bilayer on a 330 nm colloidal crystal. Despite the presence of interparticle interstices, trapping of unfused vesicles is not observed. The long-range fluidity of these bilayers is established using FRAP measurements, which indicate a 2D continuous bilayer spanning multiple beads. Quantitative analyses of these data estimate a probe diffusion coefficient of $2.1(\pm 0.4)\times 10^{-8}$ cm^2/s with a fractional mobility of 89.2 $(\pm 0.3)\%$ for POPC bilayers (doped with TR-DHPE) spread over 330 nm colloidal crystals in good agreement with the values of $1-3\times 10^{-8}$ cm^2/s reported for bilayers on planar substrates. Further analyses of these results[75] confirm that the bilayer roughly follows the colloidal topology.

For both wrinkled elastomer and colloidal crystal substrates above, the formation of fluid membranes in three-dimensional shapes prescribed by the substrate topography reflects preponderance of adhesion energy between the substrate and the bilayer. This local membrane deformation can then be understood as a result of the interplay between the substrate-membrane adhesion energy ($=-k_{ad}A$, A is the membrane-substrate interface area), lateral tension ($=\sigma A$), and curvature energy, $[=\frac{1}{2}k_b(C_1+C_2)^2A$, C_1, and C_2 are principle radii of curvature] under the constraints of overall planar topology.[51,76] For typical phosphatidylcholine (PC) lipid molecules, which are essentially cylindrical (spontaneous curvature, $C_0\sim 0$), the substrate-induced membrane bending must give rise to a net deformation.[54] A central question in this regard is to what extent the membrane can bend or follow the curvature of strongly adhering silicalike substrates before the energetic penalties result in membrane rupture, lysis, or suspension over the curved substrates[77] It appears that in the topographic regimes where the characteristic length scale for the bending energy for fluid bilayers[47] $[=(k/\sigma)^{1/2}\ \sim 10-50\ \mathrm{nm}]$ is approached in colloidal crystals and wrinkled elastomers, the membrane must abandon substrate corrugation in response to rising bending (and tension) energy penalties. However, these estimates remain experimentally unverified. Current experiments in our laboratory address this issue.

The two nonlithographic methods for forming curved supported membrane configurations illustrated above, as well as other nano- and microlithographic approaches demonstrated previously,[61,62,78] open up useful opportunities to systematically address the physical-chemical basis for the formation of curvature-niche (curvature specific lipid microenvironments wherein biochemical and biophysical processes are most likely to occur) formation and possibly their functional consequences. It is now well appreciated that in biological membranes, physical curvatures are not passive consequences of cellular activity. Rather, they represent active conformational switches to localize and induce specific membrane functions. They elicit spatial and temporal heterogeneity of function via a local control of many physical-chemical properties within the "curvature niche" of the lipid bilayer. Mechanisms for (dynamic) curvature generation in biological membranes include a variety of intrinsic and extrinsic pathways including insertion of curvature-sensitive lipids and membrane proteins, surface scaffolding by cytoskeletol (re) polymerization, protein-binding, and motor protein activity.[79,80]

Within this broad framework, several immediately useful studies using the curved model membranes can be envisaged. *First*, the model systems introduced above allow for systematic experiments toward how mesoscale membrane remodeling influences molecular distributions. For instance, studies of the determination of the role of molecular geometry and spontaneous membrane curvature onto the formation and stability of lipid bilayer membranes on curved substrates can be profoundly useful. Typical molecular shapes for lipids are characterized by their spontaneous curvature, C_0. They are broadly categorized as cylindrical (e.g., phosphatidylcholine, PC, $C_0\sim 0$), conical (e.g., lyso-PCs, $C_0>0$), and inverted-conical (e.g., phosphatidylethanolamines, PE, $C_0<0$). Free membranes of cylindrical lipids spontaneously assume planar or lamellar configurations whereas conical and inverted-conical lipids tend to favor curved geometries.[81] Several independent studies have shown that PE lipids inhibit formation of planar lamellar bilayers[82] and that in mixtures containing PE and PC lipids, PE lipids tend to concentrate at the curved boundaries.[83] 1D and 2D curved substrates described here provide simple templates to examine how membrane deformations can give rise to sorting of molecules based on their shape. Such experiments may help understand membrane polymorphism—a long-standing debate in biophysics about why biological membranes use non-bilayer forming molecules at all.[84] *Second*, these model membrane configurations provide a straightforward means to determine the effects of curved membrane geometry on membrane phase transition characteristics. The deformation of membranes induced by substrate-imposed curvatures must alter their local lateral packing densities and consequently alter intermolecular interactions between acyl tails, lipid head groups, and surrounding aqueous phase. How this membrane remodeling, together with strong substrate adhesion interactions, influences effective transition temperature and lateral fluidity[85] appears particularly interesting because of their importance on many membrane associated functions. *Third*, the abilities to template curvatures within phospholipid bilayers in defined spatial patterns also allows for the examination of how biomembranes use their curvatures to modulate lateral phase segregation and domain distributions[86] (curvature-niche formation), especially in cholesterol-enriched raftlike

phases.[87,88] The latter domains are liquid ordered and stiffer and thus should resist bending.[88] Furthermore, lateral tension in curved topologies further contributes to domain distortions by increasing line tension at the domain boundaries.[89] Indeed, a recent study by Parathasarathy and Groves[62,63,90] has shown that micrometer scale, oval-shaped, raftlike domains preferentially align in regions of low curvatures when organized as double bilayers over nanocorrugated surfaces. *Fourth*, because topological deformation of PDMS elastomers can be induced in real-time after bilayers have been allowed to equilibrate on planar topographies, the deformable elastomer based model membrane configurations should allow dynamically introduced curvatures. Such an ability will afford new measurements of how mesoscale membrane remodeling induced by curvature generation gives rise to molecular and domain redistributions or dynamic curvature-niche formation, which occur due to pervasive curvature dynamics in biological membranes.[79]

V. CONCLUSIONS

The collection of efforts summarized here suggests that deliberate coupling of lipid bilayers to substrates in supported membrane configurations offers interesting new possibilities. The efforts summarized reveal that vesicle fusion and hydration-induced spreading of lipids onto chemically and topographically structured surfaces give rise to interesting lipid patterns. These patterns can be usefully exploited for modeling many physical chemical properties of lipid bilayers, which depend on local shape, curvature morphologies, and interleaflet coupling. Chemically structured surfaces produce a lipid structure that indicates template-induced assembly of coexisting lipid mono- and bilayer structures, which reflect the underlying pattern of surface energy, wettability, and chemistry. In a construct derived using photochemically patterned silane monolayers, we find a spontaneous separation of fluid bilayer regions from the fluid monolayer regions by a controllable transition region or moat. The coexisting bi- and monolayer morphologies derived from single vesicular sources are particularly attractive for the study of leaflet-dependent biophysical processes and offer a new self-assembly strategy for synthesizing large-scale arrays of functional bilayer specific substructures including ion-channels and membrane-proteins. The use of topologically patterned surfaces similarly provides new models to design complex three-dimensional membrane topographies and curvatures. These platforms promise fundamental biophysical studies of curvature-dependent membrane processes, including dynamic membrane remodeling as well as useful bioanalytical devices for molecular separations within fluid amphiphilic membrane environments.

ACKNOWLEDGMENTS

The author thanks many colleagues and co-workers who contributed to the ideas and experiments presented in this review. Several current and past group members including Meri Amweg, Adrian Brozell, Annapoorna Butti, Ravi Butti, Sanhita Dixit, Michael Howland, Eric Kendall, Ann Oliver, Babak Sanii, Michelle Smith, Alan Szmodis, Madhuri Vinchurkar, Calvin Yang, and Chanel Yee, and collaborators including Andy Shreve (Los Alamos), Andrew Dattelbaum (Los Alamos), Jeff Brinker (Sandia), and Jay Groves (Berkeley) are thanked. Generous support from the U.S. Department of Energy Biomolecular Materials Program through a grant (DE-FG02-04ER46173) is gratefully acknowledged.

[1] E. Sackmann, Science **271**, 43 (1996).
[2] M. Tanaka and E. Sackmann, Nature (London) **437**, 656 (2005).
[3] E. T. Castellana and P. S. Cremer, Surf. Sci. Rep. **61**, 429 (2006).
[4] S. G. Boxer, Curr. Opin. Chem. Biol. **4**, 704 (2000).
[5] G. Vereb, J. Szollosi, J. Matko, P. Nagy, T. Farkas, L. Vigh, L. Matyus, T. A. Waldmann, and S. Damjanovich, Proc. Natl. Acad. Sci. U.S.A. **100**, 8053 (2003).
[6] J. T. Groves and S. G. Boxer, Acc. Chem. Res. **35**, 149 (2002); A. A. Brian and H. M. McConnell, Proc. Natl. Acad. Sci. U.S.A. **81**, 6159 (1984); H. M. McConnell, T. H. Watts, R. M. Weis, and A. A. Brian, Biochim. Biophys. Acta **864**, 95 (1986); K. D. Mossman, G. Campi, J. T. Groves, and M. L. Dustin, Science **310**, 1191 (2005).
[7] A. N. Parikh and J. T. Groves, MRS Bull. **31**, 507 (2006); B. A. Cornell, V. L. B. Braach-Maksvytis, L. G. King, P. D. J. Osman, B. Raguse, L. Wieczorek, and R. J. Pace, Nature (London) **387**, 580 (1997); H. M. Keizer, B. R. Dorvel, M. Andersson, D. Fine, R. B. Price, J. R. Long, A. Dodabalapur, I. Koper, W. Knoll, P. A. V. Anderson, and R. S. Duran, ChemBioChem **8**, 1246 (2007).
[8] H. Bayley and P. S. Cremer, Nature (London) **413**, 226 (2001); Y. Fang, A. G. Frutos, and J. Lahiri, J. Am. Chem. Soc. **124**, 2394 (2002).
[9] P. S. Cremer and S. G. Boxer, J. Phys. Chem. B **103**, 2554 (1999).
[10] I. Reviakine and A. Brisson, Langmuir **16**, 1806 (2000).
[11] C. A. Keller, K. Glasmastar, V. P. Zhdanov, and B. Kasemo, Phys. Rev. Lett. **84**, 5443 (2000).
[12] E. Kalb, S. Frey, and L. K. Tamm, Biochim. Biophys. Acta **1103**, 307 (1992); L. K. Tamm and H. M. McConnell, Biophys. J. **47**, 105 (1985).
[13] J. Nissen, S. Gritsch, G. Wiegand, and J. O. Radler, Eur. Phys. J. B **10**, 335 (1999).
[14] J. Nissen, K. Jacobs, and J. O. Radler, Phys. Rev. Lett. **86**, 1904 (2001).
[15] B. Sanii and A. N. Parikh, Soft Matter **3**, 974 (2007).
[16] V. Kiessling and L. K. Tamm, Biophys. J. **84**, 408 (2003); A. Lambacher and P. Fromherz, Appl. Phys. A: Mater. Sci. Process. **63**, 207 (1996); B. W. Koenig, S. Kruger, W. J. Orts, C. F. Majkrzak, N. F. Berk, J. V. Silverton, and K. Gawrisch, Langmuir **12**, 1343 (1996); S. J. Johnson, T. M. Bayerl, D. C. McDermott, G. W. Adam, A. R. Rennie, R. K. Thomas, and E. Sackmann, Biophys. J. **59**, 289 (1991); T. M. Bayerl and M. Bloom, *ibid.* **58**, 357 (1990).
[17] R. J. White, B. Zhang, S. Daniel, J. M. Tang, E. N. Ervin, P. S. Cremer, and H. S. White, Langmuir **22**, 10777 (2006); M. J. Higgins, M. Polcik, T. Fukuma, J. E. Sader, Y. Nakayama, and S. P. Jarvis, Biophys. J. **91**, 2532 (2006).
[18] R. J. Mashl, S. Joseph, N. R. Aluru, and E. Jakobsson, Nano Lett. **3**, 589 (2003); C. Boissiere, J. B. Brubach, A. Mermet, G. de Marzi, C. Bourgaux, E. Prouzet, and P. Roy, J. Phys. Chem. B **106**, 1032 (2002); M. C. Bellissent-Funel, J. Phys.: Condens. Matter **13**, 9165 (2001).
[19] R. P. Richter, N. Maury, and A. R. Brisson, Langmuir **21**, 299 (2005); M. Kasbauer, M. Junglas, and T. M. Bayerl, Biophys. J. **76**, 2600 (1999); M. Junglas, B. Danner, and T. M. Bayerl, Langmuir **19**, 1914 (2003).
[20] M. C. Howland, A. R. Sapuri-Butti, S. S. Dixit, A. M. Dattelbaum, A. P. Shreve, and A. N. Parikh, J. Am. Chem. Soc. **127**, 6752 (2005).
[21] P. Lenz, C. M. Ajo-Franklin, and S. G. Boxer, Langmuir **20**, 11092 (2004).
[22] J. Schmitt, B. Danner, and T. M. Bayerl, Langmuir **17**, 244 (2001); L. F. Zhang and S. Granick, J. Chem. Phys. **123**, 211104 (2005); M. Hetzer, S. Heinz, S. Grage, and T. M. Bayerl, Langmuir **14**, 982 (1998); R. Merkel, E. Sackmann, and E. Evans, J. Phys. **50**, 1535 (1989).
[23] Z. V. Feng, T. A. Spurlin, and A. A. Gewirth, Biophys. J. **88**, 2154 (2004); D. Keller, N. B. Larsen, I. M. Moller, and O. G. Mouritsen, Phys. Rev. Lett. **94**, 025701 (2005); F. Tokumasu, A. J. Jin, and J. A. Dvorak, J. Electron Microsc. **51**, 1 (2002).
[24] M. L. Wagner and L. K. Tamm, Biophys. J. **79**, 1400 (2000); E. Sackmann and M. Tanaka, Trends Biotechnol. **18**, 58 (2000); A. Graneli, J.

Rydstrom, B. Kasemo, and F. Hook, Langmuir **19**, 842 (2003).
[25]E. K. Sinner and W. Knoll, Curr. Opin. Chem. Biol. **5**, 705 (2001); J. Spinke, J. Yang, H. Wolf, M. Liley, H. Ringsdorf, and W. Knoll, Biophys. J. **63**, 1667 (1992); S. L. McArthur, M. W. Halter, V. Vogel, and D. G. Castner, Langmuir **19**, 8316 (2003).
[26]M. Geissler and Y. N. Xia, Adv. Mater. **16**, 1249 (2004).
[27]R. K. Smith, P. A. Lewis, and P. S. Weiss, Prog. Surf. Sci. **75**, 1 (2004).
[28]A. T. A. Jenkins, R. J. Bushby, S. D. Evans, W. Knoll, A. Offenhausser, and S. D. Ogier, Langmuir **18**, 3176 (2002); A. T. A. Jenkins, N. Boden, R. J. Bushby, S. D. Evans, P. F. Knowles, R. E. Miles, S. D. Ogier, H. Schonherr, and G. J. Vancso, J. Am. Chem. Soc. **121**, 5274 (1999); X. J. Han, S. N. D. Pradeep, K. Critchley, K. Sheikh, R. J. Bushby, and S. D. Evans, Chem. Eur. J. **13**, 7957 (2007); X. J. Han, K. Critchley, L. X. Zhang, S. N. D. Pradeep, R. J. Bushby, and S. D. Evans, Langmuir **23**, 1354 (2007); C. Duschl, M. Liley, G. Corradin, and H. Vogel, Biophys. J. **67**, 1229 (1994).
[29]A. L. Plant, M. Gueguetchkeri, and W. Yap, Biophys. J. **67**, 1126 (1994).
[30]A. L. Plant, Langmuir **15**, 5128 (1999).
[31]A. N. Parikh, J. D. Beers, A. P. Shreve, and B. I. Swanson, Langmuir **15**, 5369 (1999).
[32]J. C. Love, L. A. Estroff, J. K. Kriebel, R. G. Nuzzo, and G. M. Whitesides, Chem. Rev. **105**, 1103 (2005).
[33]Y. N. Xia and G. M. Whitesides, Annu. Rev. Mater. Sci. **28**, 153 (1998).
[34]R. Lipowsky and U. Seifert, Mol. Cryst. Liq. Cryst. **202**, 17 (1991); U. Seifert and R. Lipowsky, Phys. Rev. A **42**, 4768 (1990); M. Twardowski and R. G. Nuzzo, Langmuir **19**, 9781 (2003).
[35]V. I. Silin, H. Wieder, J. T. Woodward, G. Valincius, A. Offenhausser, and A. L. Plant, J. Am. Chem. Soc. **124**, 14676 (2002).
[36]E. Reimhult, F. Hook, and B. Kasemo, Langmuir **19**, 1681 (2003).
[37]J. Raedler, H. Strey, and E. Sackmann, Langmuir **11**, 4539 (1995); J. B. Hubbard, V. Silin, and A. L. Plant, Biophys. Chem. **75**, 163 (1998).
[38]P. Frantz and S. Granick, Langmuir **8**, 1176 (1992).
[39]M. Ahlers, W. Muller, A. Reichert, H. Ringsdorf, and J. Venzmer, Angew. Chem. Int. Ed. Engl. **29**, 1269 (1990).
[40]P. S. Swain and D. Andelman, Langmuir **15**, 8902 (1999); P. S. Swain and D. Andelman, Phys. Rev. E **63**, 051911 (2001).
[41]J. M. Calvert, M. S. Chen, C. S. Dulcey, J. H. Georger, M. C. Peckerar, J. M. Schnur, and P. E. Schoen, J. Electrochem. Soc. **139**, 1677 (1992).
[42]C. S. Dulcey, J. H. Georger, V. Krauthamer, D. A. Stenger, T. L. Fare, and J. M. Calvert, Science **252**, 551 (1991).
[43]J. B. Brzoska, N. Shahidzadeh, and F. Rondelez, Nature (London) **360**, 719 (1992); A. N. Parikh, D. L. Allara, I. B. Azouz, and F. Rondelez, J. Phys. Chem. **98**, 7577 (1994).
[44]G. P. Lopez, H. A. Biebuyck, C. D. Frisbie, and G. M. Whitesides, Science **260**, 647 (1993).
[45]D. Axelrod, D. E. Koppel, J. Schlessinger, E. Elson, and W. W. Webb, Biophys. J. **16**, 1055 (1976).
[46]J. O. Radler, S. Radiman, A. Devallera, and C. Toprakcioglu, Physica B **156-157**, 398 (1989).
[47]M. Deserno, J. Phys.: Condens. Matter **16**, S2061 (2004).
[48]J. Zimmerberg and L. V. Chernomordik, Adv. Drug Deliv. Rev. **38**, 197 (1999); F. S. Cohen and G. B. Melikyan, J. Membr. Biol. **199**, 1 (2004); H. Garoff, R. Hewson, and D. J. E. Opstelten, Microbiol. Mol. Biol. Rev. **62**, 1171 (1998).
[49]A. Boulbitch, Europhys. Lett. **59**, 910 (2002); C. Tordeux and J. B. Fournier, Langmuir **16**, 2991 (2000).
[50]I. Koltover, J. O. Radler, and C. R. Safinya, Phys. Rev. Lett. **82**, 1991 (1999); C. Dietrich, M. Angelova, and B. Pouligny, J. Phys. II **7**, 1651 (1997).
[51]U. Seifert, Adv. Phys. **46**, 13 (1997).
[52]M. B. Schneider, J. T. Jenkins, and W. W. Webb, J. Phys. **45**, 1457 (1984).
[53]P. Girard, J. Prost, and P. Bassereau, Phys. Rev. Lett. **94**, 088102 (2005); J. D. Cortese, B. Schwab, C. Frieden, and E. L. Elson, Proc. Natl. Acad. Sci. U.S.A. **86**, 5773 (1989).
[54]S. S. Dixit, A. Szmodis, and A. N. Parikh, ChemPhysChem **7**, 1678 (2006).
[55]M. Deserno and T. Bickel, Europhys. Lett. **62**, 767 (2003).
[56]T. H. Yang, C. K. Yee, M. L. Amweg, S. Singh, E. L. Kendall, A. M. Dattelbaum, A. P. Shreve, C. J. Brinker, and A. N. Parikh, Nano Lett. **7**, 2446 (2007).
[57]G. A. Woolley and B. A. Wallace, J. Membr. Biol. **129**, 109 (1992).
[58]G. Wirnsberger, B. J. Scott, and G. D. Stucky, Chem. Commun. (Cambridge) **2001**, 119 (2001).
[59]A. M. Dattelbaum, M. L. Amweg, L. E. Ecke, C. K. Yee, A. P. Shreve, and A. N. Parikh, Nano Lett. **3**, 719 (2003).
[60]M. A. Meitl, Z. T. Zhu, V. Kumar, K. J. Lee, X. Feng, Y. Y. Huang, I. Adesida, R. G. Nuzzo, and J. A. Rogers, Nat. Mater. **5**, 33 (2006); R. J. Jackman, S. T. Brittain, A. Adams, M. G. Prentiss, and G. M. Whitesides, Science **280**, 2089 (1998).
[61]J. T. Groves, Annu. Rev. Phys. Chem. **58**, 697 (2007).
[62]R. Parthasarathy and J. T. Groves, Soft Matter **3**, 24 (2007).
[63]R. Parthasarathy, C. H. Yu, and J. T. Groves, Langmuir **22**, 5095 (2006).
[64]J. Huang, M. Juszkiewicz, W. H. de Jeu, E. Cerda, T. Emrick, N. Menon, and T. P. Russell, Science **317**, 650 (2007); E. Cerda and L. Mahadevan, Phys. Rev. Lett. **90**, 074302 (2003); N. Bowden, W. T. S. Huck, K. E. Paul, and G. M. Whitesides, Appl. Phys. Lett. **75**, 2557 (1999).
[65]K. Efimenko, M. Rackaitis, E. Manias, A. Vaziri, L. Mahadevan, and J. Genzer, Nat. Mater. **4**, 293 (2005).
[66]K. Efimenko, W. E. Wallace, and J. Genzer, J. Colloid Interface Sci. **254**, 306 (2002).
[67]N. Bowden, S. Brittain, A. G. Evans, J. W. Hutchinson, and G. M. Whitesides, Nature (London) **393**, 146 (1998).
[68]N. Bowden, W. T. S. Huck, K. E. Paul, and G. M. Whitesides, Appl. Phys. Lett. **75**, 2557 (1999).
[69]B. Sanii, A. M. Smith, R. Butti, A. M. Brozell, and A. N. Parikh (submitted).
[70]V. L. Colvin, MRS Bull. **26**, 637 (2001); P. Jiang, J. F. Bertone, K. S. Hwang, and V. L. Colvin, Chem. Mater. **11**, 2132 (1999); A. Blanco, E. Chomski, S. Grabtchak, M. Ibisate, S. John, S. W. Leonard, C. Lopez, F. Meseguer, H. Miguez, J. P. Mondia, G. A. Ozin, O. Toader, and H. M. van Driel, Nature (London) **405**, 437 (2000).
[71]Y. D. Yin, Y. Lu, B. Gates, and Y. N. Xia, J. Am. Chem. Soc. **123**, 8718 (2001).
[72]S. H. Park, D. Qin, and Y. Xia, Adv. Mater. **10**, 1028 (1998).
[73]A. M. Brozell, M. A. Muha, and A. N. Parikh, Langmuir **21**, 11588 (2005).
[74]S. C. Glotzer and M. J. Solomon, Nat. Mater. **6**, 557 (2007); H. Y. Chen, J. M. Rouillard, E. Gulari, and J. Lahann, Proc. Natl. Acad. Sci. U.S.A. **104**, 11173 (2007); S. Venkatesh, P. Jiang, and B. Jiang, Langmuir **23**, 8231 (2007).
[75]A. M. Brozell, M. A. Muha, B. Sanii, and A. N. Parikh, J. Am. Chem. Soc. **128**, 62 (2006).
[76]M. Hamm and M. M. Kozlov, Eur. Phys. J. E **3**, 323 (2000); T. R. Weikl, D. Andelman, S. Komura, and R. Lipowsky, *ibid.* **8**, 59 (2002).
[77]A. Boulbitch, Europhys. Lett. **59**, 910 (2002).
[78]T. Y. Yoon, C. Jeong, S. W. Lee, J. H. Kim, M. C. Choi, S. J. Kim, M. W. Kim, and S. D. Lee, Nat. Mater. **5**, 281 (2006).
[79]H. T. McMahon and J. L. Gallop, Nature (London) **438**, 590 (2005); J. Zimmerberg and M. M. Kozlov, Nat. Rev. Mol. Cell Biol. **7**, 9 (2006).
[80]V. Vogel and M. Sheetz, Nat. Rev. Mol. Cell Biol. **7**, 265 (2006).
[81]I. R. Cooke and M. Deserno, Biophys. J. **91**, 487 (2006).
[82]T. J. McIntosh, Chem. Phys. Lipids **81**, 117 (1996); L. Chernomordik, *ibid.* **81**, 203 (1996); S. M. Gruner, Proc. Natl. Acad. Sci. U.S.A. **82**, 3665 (1985).
[83]C. Hamai, T. L. Yang, S. Kataoka, P. S. Cremer, and S. M. Musser, Biophys. J. **90**, 1241 (2006).
[84]R. M. Epand, Biochim. Biophys. Acta **1376**, 353 (1998); B. deKruijff, Nature (London) **386**, 129 (1997); I. Simidjiev, S. Stoylova, H. Amenitsch, T. Javorfi, L. Mustardy, P. Laggner, A. Holzenburg, and G. Garab, Proc. Natl. Acad. Sci. U.S.A. **97**, 1473 (2000); K. C. Huang, R. Mukhopadhyay, and N. S. Wingreen, PLoS Comput. Biol. **2**, e151 (2006).
[85]M. C. Giocondi, L. Pacheco, P. E. Milhiet, and C. Le Grimellec, Ultramicroscopy **86**, 151 (2001); T. Heimburg, Biophys. J. **78**, 1154 (2000).
[86]W. B. Huttner and J. Zimmerberg, Curr. Opin. Cell Biol. **13**, 478 (2001).
[87]W. H. Binder, V. Barragan, and F. M. Menger, Angew. Chem. Int. Ed. **42**, 5802 (2003); K. Simons and E. Ikonen, Nature (London) **387**, 569 (1997).
[88]K. Simons and W. L. C. Vaz, Annu. Rev. Biophys. Biomol. Struct. **33**, 269 (2004).
[89]S. A. Akimov, P. I. Kuzmin, J. Zimmerberg, and F. S. Cohen, Phys. Rev. E **75**, 011919 2007).
[90]A. G. Lee, Curr. Biol. **10**, R377 (2000).